ISSN 1990-519X, Cell and Tissue Biology, 2016, Vol. 10, No. 3, pp. 233–241. © Pleiades Publishing, Ltd., 2016.
Original Russian Text © S.N. Pleskova, E.N. Aybeke, E. Bourillot, E. Lesniewska, 2016, published in Tsitologiya, 2016, Vol. 58, No. 2, pp. 120–128.

Characteristics of Morphological Differences of Detergent-Resistant Membrane Domains Isolated from Different Cells and Investigated by Atomic Force Microscopy

S. N. Pleskova[a, b, *], E. N. Aybeke[a], E. Bourillot[a], and E. Lesniewska[a]

[a] *Carnot Interdisciplinary Laboratory of Burgundy, University of Burgundy, Dijon, France 21000*

[b] *Research and Education Center Physics of Solid State Nanostructures, Lobachevsky State University of Nizhny Novgorod, Nizhny Novgorod, 603950 Russia*

**e-mail: pleskova@mail.ru*

Received September 23, 2015

Abstract—Planar rafts and caveolae are specific membrane clusters that contain high concentrations of cholesterol and lipids consisting of saturated fatty acids. These clusters are resistant to detergents and are known as "detergent-resistant membrane domains" (DRMs). Their morphology and size were studied by atomic force microscopy (AFM). Planar rafts extracted by Lubrol WX from monocytes of healthy donors are 150.6 ± 68.6 nm in diameter and 5.7 ± 2.9 nm in height, while caveolae are 87.3 ± 46.1 nm in diameter and 9.4 ± 5.4 nm in height. Significant differences in size and morphology were found between DRMs isolated from monocytes of healthy donors and patients with myocardial infarction, as well as between DRMs of monocytes and endothelial cells. The morphology dynamics of the isolated planar rafts and caveolae indicates that they quickly aggregate during storage; therefore, in order to assess the actual DRM size and morphology it is necessary to investigate them immediately after isolation.

Keywords: planar rafts, caveolae, morphology, size, atomic force microscopy

DOI: 10.1134/S1990519X16030081

INTRODUCTION

The asymmetry of membranes plays a key role in the preservation and maintenance of cellular homeostasis. Functional responses of cells are largely due to rafts (microdomains), which are highly dynamic structures of the membrane lipid bilayer characterized by a specific lipid and protein composition with a predominance of cholesterol, sphingolipids, and specific transmembrane proteins (Korade and Kenworthy, 2008). Rafts have been shown to be involved in such processes as the assembly of signaling molecules (Sheets et al., 1999; Drevot et al., 2002; Gohlke et al., 2010), the regulation of ion channel and impulse transmission through the nervous system (Dart, 2010; Levitan et al., 2010), and membrane fluidity and membrane protein trafficking (Melser et al., 2011). Moreover, rafts regulate physiological and pathophysiological processes at the cellular level. In some cases, they contribute to the realization of protective mechanisms (Marin et al., 2012); in others, on the contrary, they increase the sensitivity of the cells to invasion (Huang et al., 2011). Signaling complexes that induce cell proliferation when they bind to specific ligands can be assembled on raft platforms (Scuderi et al., 2011; Sowa, 2011); in other cases, protein complexes that are sensitive to proapoptotic activation are concentrated in the rafts (Gajate et al., 2009; Gajate and Mollinedo, 2011).

There are two types of rafts: planar lipid rafts, which are defined as "noncaveolar structures," and rafts known as "caveolae" (Pleskova and Pudovkina, 2013). Planar rafts have specific morphological features and do not form invagination (Staubach and Hanisch, 2011), while caveolae are formed through polymerization of the caveolin, a hairpinlike palmitoylated integral membrane protein that strongly and stably binds to cholesterol (Smart et al, 1999).

The use of detergents for extraction of rafts and their investigation in vitro is a convenient and widely used procedure, which enables one to analyze the structural and functional features of DRMs. Moreover, the combination of zonal centrifugation through sucrose gradient (after detergent treatment of the cells) with Western blot is useful for the determination of the proteins that are specific markers of microdomains. Such a combination of methods enables one to analyze the differences between planar rafts and caveolae with high accuracy (Salvary et al., 2012). In particular, it has been shown that the use of Lubrol WX

[1] *Abbreviations:* AFM—atomic force microscopy, DRM—detergent-resistant membrane domains, LDL—low density lipoproteins, MI—myocardial infarction, HUVEC—human umbilical vein endothelial cells.

as a detergent enables one to maximally preserve cholesterol and sphingomyelin in the lipid rafts, unlike Triton X-100 and sodium carbonate (Salvary et al., 2012). In addition, the use of sucrose gradient enables one to isolate fractions of the planar rafts and caveolae enriched in cholesterol and sphingomyelin.

However, lipid analysis and Western blot allow one to determine only the DRM biochemical composition, but not present the morphology of the isolated planar rafts and caveolae. To evaluate DRM morphology, we used atomic force microscopy (AFM), which allows one not only to observe cellular and subcellular structures (including the rafts) in the buffer (under the conditions close to physiological), but also to conduct morphometry with high accuracy (Pleskova, 2011).

The main principle of AFM is the evaluation of interatomic interaction forces between the probe and the sample during the scanning process. The probe is rigidly fixed on the cantilever, an elastic lever, deflections of which are detected by an optical microscope system. The main physical characteristics of the cantilevers are rigidity k and resonance frequency f_0. When the probe passes over the DRM surface, it interaction with the biological sample causes cantilever deflection, which corresponds to the topography of the investigated surface. Flexion or torsion of the cantilever is registered by an optical microscope system (a laser beam reflected off the cantilever tip into the center of a four-section photodiode). This signal is detected and corrected in a feedback system. The information obtained from the probe passing over the surface of the scanned object is written as an array, which can be easily transformed into a real 3D image of the investigated object. Since the probe interacts with all the structures during the investigation of the surface, the final result of scanning is the exact morphology of the object. The fact that AFM allows one to study cells and subcellular structures in the native environment (buffers, media) and, thus, to monitor living cells (either isolated subcellular structures) and their morphological changes in response to various effects in real time at a resolution that is not inferior to that of scanning and transmission electron microscopy is the main advantage of this method.

In the present study, we focused on three main objectives: 1) identifying the morphological differences between planar rafts and caveolae, 2) finding the morphological features of monocyte DRMs of patients with myocardial infarction (MI), and 3) examining the morphological features of planar rafts and caveolae isolated from different cells. Since many researchers investigate DRM morphology not only on the day of isolation, but also after 2–3 days, we formulated an additional methodological problem to trace the changes in the morphology of planar rafts and caveolae 5–7 days after isolation, with aliquots being are stored under standard conditions at 4°C.

MATERIALS AND METHODS

Isolation of cells. Monocytes were isolated from venous blood of healthy donors by the Ficoll–Hypaque gradient (Pharmacia, Sweden), after which the cells were washed four times with phosphate-buffered saline (PBS) to remove of platelets. The fraction of monocytes $CD14^+/CD16^+$ was concentrated by a special kit of monoclonal antibodies (Miltenyi Biotec, Bergisch-Gladbach, Germany). Monocytes from venous blood of patients with MI were isolated similarly. We used the blood of patients younger than 75 years of age who had been diagnosed with acute MI for the first time. Endothelial cells of human umbilical vein (HUVEC) were isolated from umbilical cords by collagenase treatment (Roche, Switzerland). Initially, the veins were washed with 150 mL of PBS, after which they were filled with a solution of 0.1% collagenase (Roche, Switzerland). After incubation (15 min, 37°C), the cells were collected by centrifugation (200 g, 10 min). The cell pellet was resuspended in RPMI-1640 medium (Sigma-Aldrich, United States) containing 20% fetal calf serum (Lonza, Verviers, Belgium), 15 mmol/L HEPES (Thermo Fisher Scientific, United States), 2 mmol/L L-glutamine (Thermo Fisher Scientific, United States), and 100 mg/mL streptomycin (Invitrogen, United States) and transferred to a Petri dish. After the formation of a homogeneous cell layer (at 37°C and 5% CO_2), the cells were removed with a mixture of trypsin (Sigma-Aldrich, United States) and EDTA (1 : 1) and were subcultured to obtain the second passage. In all experiments, cells of each of the two passages were used separately.

Isolation of DRMs. The planar rafts and caveolae were isolated from the cells in a MBS buffer (1 mL) using 0.1% Lubrol WX (Serva, France) as a detergent, which was added to the buffer with the cells on ice. The incubation time was 30 min. This was followed by lysate homogenization using a homogenizer (Dounce homogenizer, Sigma-Aldrich, United States), and homogenized lysate was mixed with 90% sucrose solution to a final concentration of 45%. After this, zonal centrifugation was carried out at a sucrose density gradient of 45–5% (20 h, 39000 g, SW41, Beckman Coulter, United States). As a result of the centrifugation, 12 fractions were obtained, of which the second and fifth fractions were most enriched in cholesterol and sphingomyelin (see Results).

Lipid analysis. For lipid extraction, 5 mL of methanol and 2.5 mL of chloroform were added to 2 mL of the obtained rafts, resulting in the formation of a single phase. The mixture was kept at room temperature with periodic shaking. Then, 7.5 mL of chloroform and 1.75 mL of KCl were added to a final concentration of 0.2 M to separate the phases. After stirring, the samples were centrifuged (600 g, 10 min). The lower chloroform phase containing the lipids was evaporated, and the residue was redissolved in a mixture of metha-

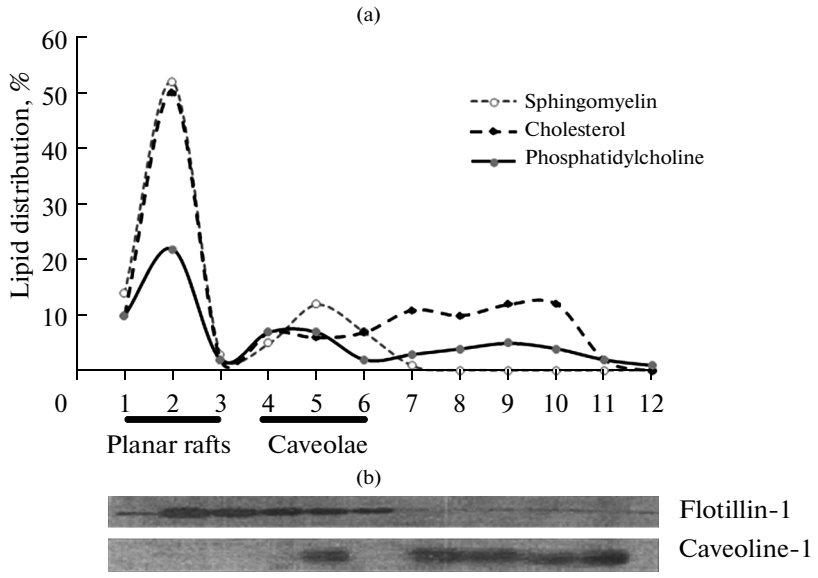

Fig. 1. Distribution of sphingomyelin, cholesterol and phosphatidylcholine in the lipid fractions separated by sucrose gradient, which were extracted with Lubrol WX from the membranes of monocytes (a), and parallel evaluation of flotillin-1 and caveoline-1 content in the same fractions, performed using Western blot analysis (b). The sphingomyelin/phosphatidylcholine ratio is maximum in fractions 2 and 5, the presence of flotillin-1 is typical for fraction 2, and the presence of caveoline-1 is typical for fraction 5. Fractions 1, 2, and 3 contain planar rafts; fractions 4, 5, and 6 contain caveolae.

nol and chloroform and, then, analyzed by thin layer chromatography. Iron thiocyanate (Enzymatic colorimetric kit, Wako Chemicals, Germany) was used to determine the phospholipid content. An Amplex red cholesterol assay kit (Invitrogen, United States) was used for quantitative determination of cholesterol.

Western blot analysis was used for protein determination in the isolated fractions. Each fraction (6 μL) was mixed with 4x Laemmli sample buffer and boiled for 5 min. The proteins were separated electrophoretically in 12% polyacrylamide gel containing sodium dodecyl sulfate and, then, transferred to nitrocellulose membrane (Whatman, United States). After the blocking of nonspecific binding with 5% dry milk in PBS containing 0.1% Tween-20 for 60 min, the membranes were incubated (18 h, 4°C) with monoclonal antibodies against flotillin-1 (Santa Cruz, United States) and caveolin-1 (Transduction Laboratories, United States) (dilution 1 : 600), washed twice with PBS and Tween, and incubated (60 min, 4°C) with secondary antimouse or antirabbit antibodies conjugated with horseradish peroxidase (1 : 5000) (Santa Cruz, United States). The membrane was washed twice with PBS and Tween, and, then, immunodetection was performed using an ECL detection kit (Amersham, United States).

AFM. DRM fractions 2 and 5 (20 μL in PBS) were placed on freshly cleaved mica surfaces (RIBM mica, Japan), and the upper mica layer was separated using a sticky tape. After sedimentation and spontaneous adsorption of DRMs to the mica (20 min, 24°C), their morphology was investigated by multimodal AFM (Nanoscope multimode 8, Bruker). Cantilevers with characteristics optimal for DRM investigation were used: DNP-S (Bruker) with resonance frequency f_0 = 40–75 kHz and rigidity k = 0.4–12 N/m.

Statistical analysis. Comparison of the variances for the average values of the control and experimental data was performed using Student's t-test for independent samples. The differences between two samples were considered statistically significant at $p < 0.05$. The limits of the normal distribution of quantitative measures were predetermined using the Shapiro–Wilk test. Origin Pro 8 software was used for the statistical analysis.

RESULTS

DRM isolation by the detergent treatment of the cells on ice and subsequent zonal centrifugation resulted in 12 fractions. The results of the study on the lipid composition and marker proteins of isolated fractions are shown in Fig. 1. According to the lipid analysis, fractions 2 and 5 were the most enriched in cholesterol and sphingomyelin, moreover, sphingomyelin/phosphatidylcholine and cholesterol/phosphatidylcholine ratios were maximum for fraction 2, which is typical for liquid-ordered phases, in particular, for rafts (de Almieda et al., 2003). Only the ratio of sphingomyelin/phosphatidylcholine was shifted toward sphingomyelin for fraction 5, while the cholesterol and phosphatidylcholine levels were similar. Thus, during DRM isolation by Lubrol WX, according to lipid analysis, planar rafts (fractions 1, 2, 3), caveo-

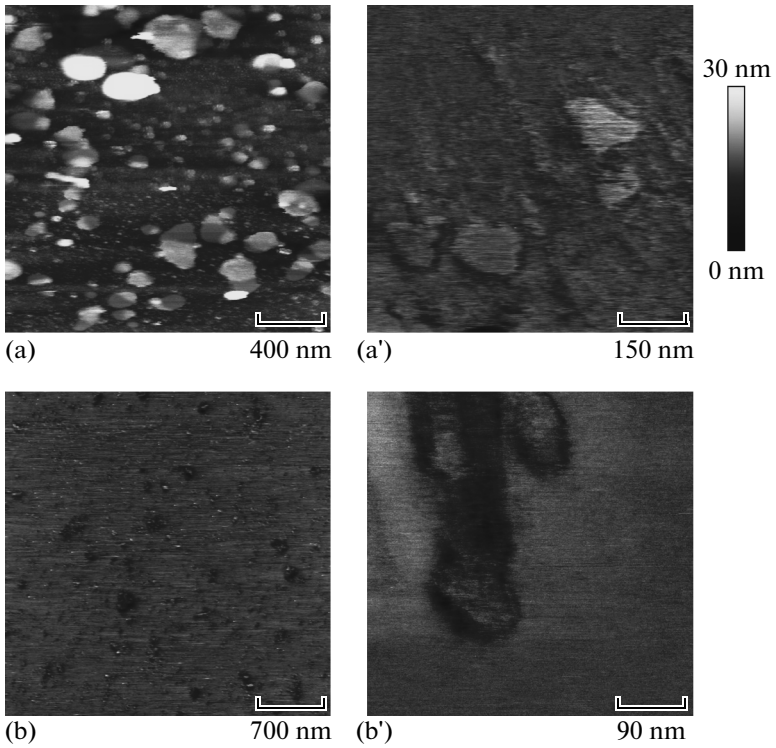

Fig. 2. Morphology of planar rafts (a, a') and caveolae (b, b') at the first day after the isolation from monocytes. (a, b) A large scanning field; (a', b') image of planar rafts (flat form) and caveolae (flask shaped form), respectively. The scan obtained on the mica surface by atomic force microscopy (Bruker). The height scale shows heights of objects: lighter shades correspond to higher objects.

lae (fractions 4, 5, 6), and nonraft fractions (from 7 to 12) were obtained.

In all the experiments, fraction 2 was used as a source of planar rafts and fraction 5 as a source of caveolae, since the maximum ratio of sphingomyelin to phosphatidylcholine was found in them, which is typical for the rafts. Furthermore, the maximum flotillin-1 (the marker protein of the planar rafts) content was found in fraction 2, while the maximum caveolin-1 (the main caveola marker) content was found in fraction 5 (Fig. 1). Individual samples of fractions 2 and 5 were applied to the surface of freshly cleaved mica. DRM adsorption took place on the support, but the position on the surface was different for the planar rafts and caveolae.

The morphology of the planar rafts and caveolae is shown in Fig. 2. Due to a flat structure, homogeneous interaction of all the points of their bottom surface with mica was typical for planar rafts (Fig. 2a); therefore, lying on the support, they retained a flat morphology (Fig. 2a'), but even on the first day of investigation some aggregation of the planar rafts could be observed (Fig. 2a). In the case of caveolae, the presence of caveolin-1 resulted in preservation of a flask-shaped structure. Thus, caveolae were adsorbed on mica in two ways: either they descended down the sides, forming the morphology of a "flask" (Fig. 2b'), or were connected with mica at the upper part that is opened on the cell, forming the morphology of a "dome" (see Fig. 4c). In the first case, the side part of caveolae was scanned; in the second, the lower part was (invaginated into the cell).

In addition, morphometric study of DRMs was carried out. Two main parameters, height and diameter, were defined. The surface profile, oriented in the direction of the scanning, was constructed to determine the height (Fig. 3a). The mica level was used as the lower point ("0" on the *OY* axis) and the highest point of DRMs as the upper point. In the case of caveola height investigation, only the height of the "dome-shaped" structures were examined to avoid artifacts. The direction of measurements was chosen arbitrarily to determine the DRM diameter, and clipping planes were placed at half-height (Fig. 3b) to avoid the convolution effect.

Morphologically speaking, planar rafts are substantially different from caveolae. First, the shape and the dimensions of the planar rafts vary over a wide range, while the morphology of caveolae is quite monotonous. The diameter variation coefficient is 0.47 and 0.21 for planar rafts and caveolae, respectively. Second, the average diameter of the planar rafts is larger than that of caveolae, while height of caveolae are bigger than the planar rafts (see table). Third, the morphological differences between the planar rafts (Fig. 2a'), having a flat shape, and caveolae, forming

flask-shaped structures (Fig. 2b'), are obvious in the enlarged scans.

A comparison of the shape and dimensions of the planar rafts and caveolae isolated from monocytes of the healthy donors and patients with myocardial infarction is shown in Fig. 4. The planar rafts isolated from monocytes of patients suffering MI have the same height as planar rafts of monocytes isolated from healthy donors: 5.8 ± 1.7 nm ($n = 18$, $p > 0.05$), but their diameter is significantly smaller: 63 ± 8.2 nm ($n = 18$, $p < 0.05$) (the results of the morphometry for the planar rafts of healthy donors are shown in the table). Morphological differences are fairly easy to determine: while the rafts isolated from the healthy donor cells has clear classical form of rafts or islands, the planar rafts of the patients after MI predominately have the form of an open ring (Fig. 4b). A decrease in the size in the case of MI is typical also for caveolae: their height is reduced in comparison with the caveolae isolated from monocytes of the healthy donors, and it is equal to 6.6 ± 2.6 nm ($n = 81$, $p < 0.05$). Only a tendency to decrease is observed for the diameter: 81.9 ± 37.6 nm ($n = 81$, $p > 0.05$) (the results of the morphometry for healthy donor caveolae are presented in the table). In addition caveolae, isolated from monocytes of the patients with MI possess a clear tendency to aggregate (Fig. 4d). Furthermore, they generally could form a monolayer on the surface of mica (Fig. 4e).

There are no less significant differences between the DMD isolated from different cells. Figure 5 shows planar rafts and caveolae isolated from other human cells (HUVEC). It follows from comparison of Fig. 2a (the morphology of the planar rafts from monocytes) and Fig. 5a (the morphology of the planar rafts from HUVEC), as well as Figs. 2b and 4c (the morphology of caveolae from monocytes) and Fig. 5b (the morphology of caveolae from HUVEC) that the corresponding structures are quite different in different cell types. The results demonstrate that planar rafts isolated from HUVEC form large confluent structures having a complicated morphology. In this case, it is not proper to discuss the diameter of large platforms; rather, one can determine their transverse size. The transverse size of the planar rafts isolated from HUVEC is 200 ± 61.7 nm, versus 150.6 ± 68.6 nm for monocyte rafts ($n = 38$, $p < 0.05$); moreover, their height is greater than that of similar structures isolated from monocytes and is 7 ± 2.3 nm versus 5.7 ± 2.9 nm for monocyte rafts ($n = 38$, $p < 0.05$). In contrast, a significant decrease in the size was detected for HUVEC

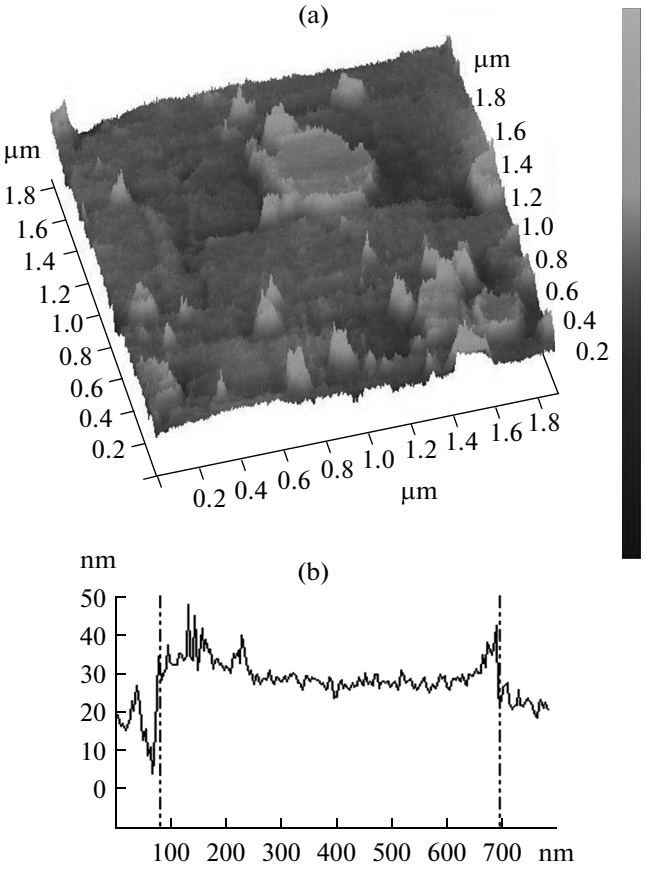

Fig. 3. Morphometry of planar rafts: AFM scan of planar rafts on the fifth day of the observation (a) and profile of planar raft, in which the cross section is oriented in the direction of the scanning (b). Clipping planes are denoted by dashed line. In this case, they show that the diameter of the studied planar raft is 600 nm (b).

Dynamics of main morphological parameters of DRMs isolated from monocytes of healthy donors

Parameter	Size, nm						
	planar rafts				caveolae		
	time, days				time, days		
	1 (control, $n = 74$)	2 ($n = 68$)	3 ($n = 61$)	5 ($n = 11$)	1 ($n = 61$)	5 ($n = 10$)	7 ($n = 45$)
Height	5.7 ± 2.9	13.0 ± 1.9[a]	5.9 ± 2.2[a]	30.2 ± 4.3[a]	9.4 ± 5.4	43.7 ± 25.2[a]	10.4 ± 4.8[a]
Diameter	150.6 ± 68.6	158.4 ± 95.2[a]	263.9 ± 168.9[a]	245.0 ± 170.0[a]	87.3 ± 46.1	93.9 ± 54.4[a]	98.4 ± 53.8[a]

[a] $p < 0.05$—difference is significant relative to data on the 1st day; n—number of measurements.

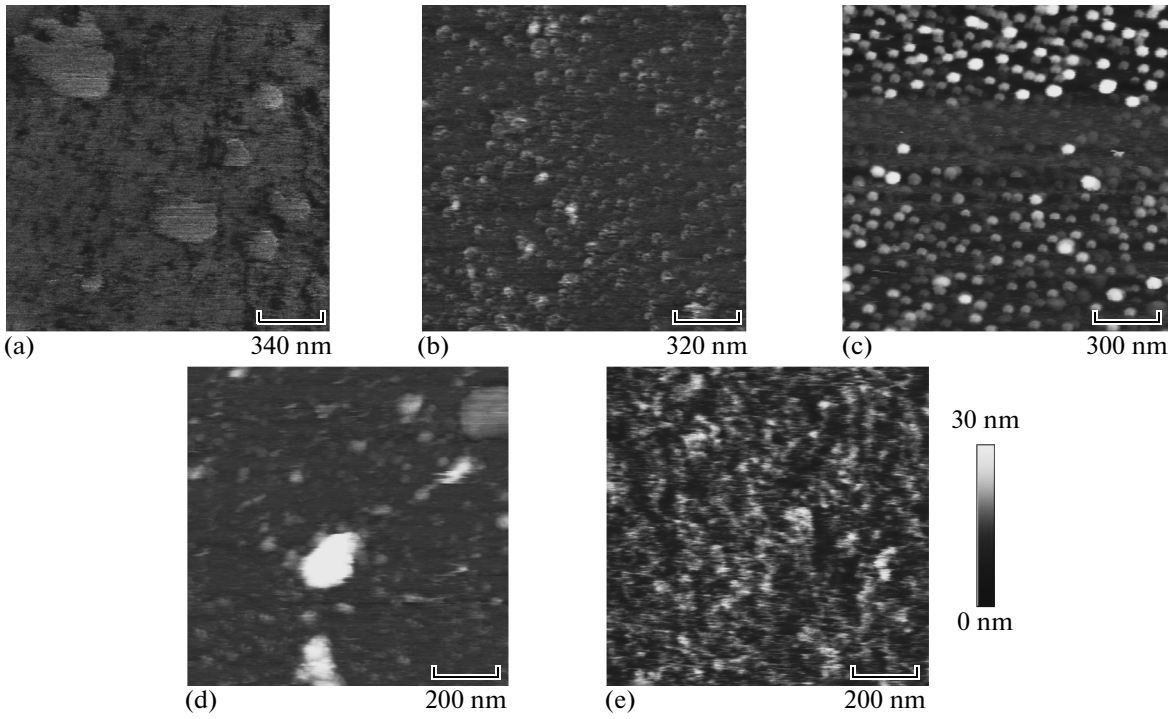

Fig. 4. Morphology of detergent-resistant membrane domains isolated from monocytes of healthy donors (a, c) and a patient suffering from myocardial infarction (MI), (b, d, e). (a, b) Planar rafts of healthy donors and the patient with MI, respectively; (c, d) caveolae of healthy donors and a patient with MI, respectively; (e) caveolae form a monolayer on the surface of mica under MI. The height scale shows heights of objects: lighter shades correspond to higher objects.

caveolae compared with DRMs, isolated from monocytes. In particular, the average diameter of HUVEC caveolae is 45.1 ± 7.1 nm versus 87.3 ± 46.1 nm for monocytes ($n = 22$, $p < 0.05$), while average height is 7.8 ± 2.8 nm versus 9.4 ± 5.4 for monocytes ($n = 22$, $p < 0.05$).

Dynamics of the main parameters of the planar rafts and caveolae (diameter and height) are shown in the table. Fractions 2 and 5 isolated from healthy donor monocytes were kept as aliquots in a refrigerator. For daily observations, two or three aliquots were used. A significant increase in the size due to aggregation is observed at the second day. The greatest DRM height (of both the planar rafts and caveolae) was registered on the fifth day of the observation, and the maximum diameter was detected on the third day for planar rafts and on the seventh day for caveolae (see table).

DISCUSSION

The extreme polymorphism of the planar rafts is noteworthy. Obviously, polymorphism is determined by raft evolution, since initially nanodomains are formed; then, during lateral migration, microdomains appear; and, finally, large clusters or platforms are formed (Quinn and Wolf, 2009). Thus, when a detergent is used, extracted fractions may consist of DRMs, which are at different stages of their evolution; it is manifested in different morphology of the planar rafts on the support. The thickness of the lipid bilayer based on the approximate estimates is 4 nm. The height of the raft exceeds the height of the surrounding bilayer. In our case, the measured height of the planar rafts is also slightly higher than 4 nm.

It has been shown (Salvary et al, 2012) that the use of Lubrol WX as a detergent promotes the maximum preservation of cholesterol, sphingomyelin and caveolin-1 (the marker protein of caveolae) as parts of DRMs. Our results show that it is the maximum preservation of caveolin, apparently, leads to the preservation of the flask shaped form of caveolae (Figs. 2b, 4c). The height of the extracted caveolae is substantially greater than the height of the isolated planar rafts. According to the Western blot results, Lubrol WX does not remove the main marker proteins (Salvary et al, 2012), neither flotillin-1 of the planar rafts nor caveolin-1 of the caveolae. At the same time, the use of this detergent makes DRMs free of cytoskeleton elements, as is shown by AFM data. Thus, the differences in height are, probably, caused by caveolin polymerization.

It is an interesting fact that significant differences in the morphology and size of planar rafts and caveolae isolated from monocytes of healthy people and patients after MI were identified. Monocytosis is a widely known fact in atherosclerosis and MI. Monocytes are recruited from bone marrow and migrate into

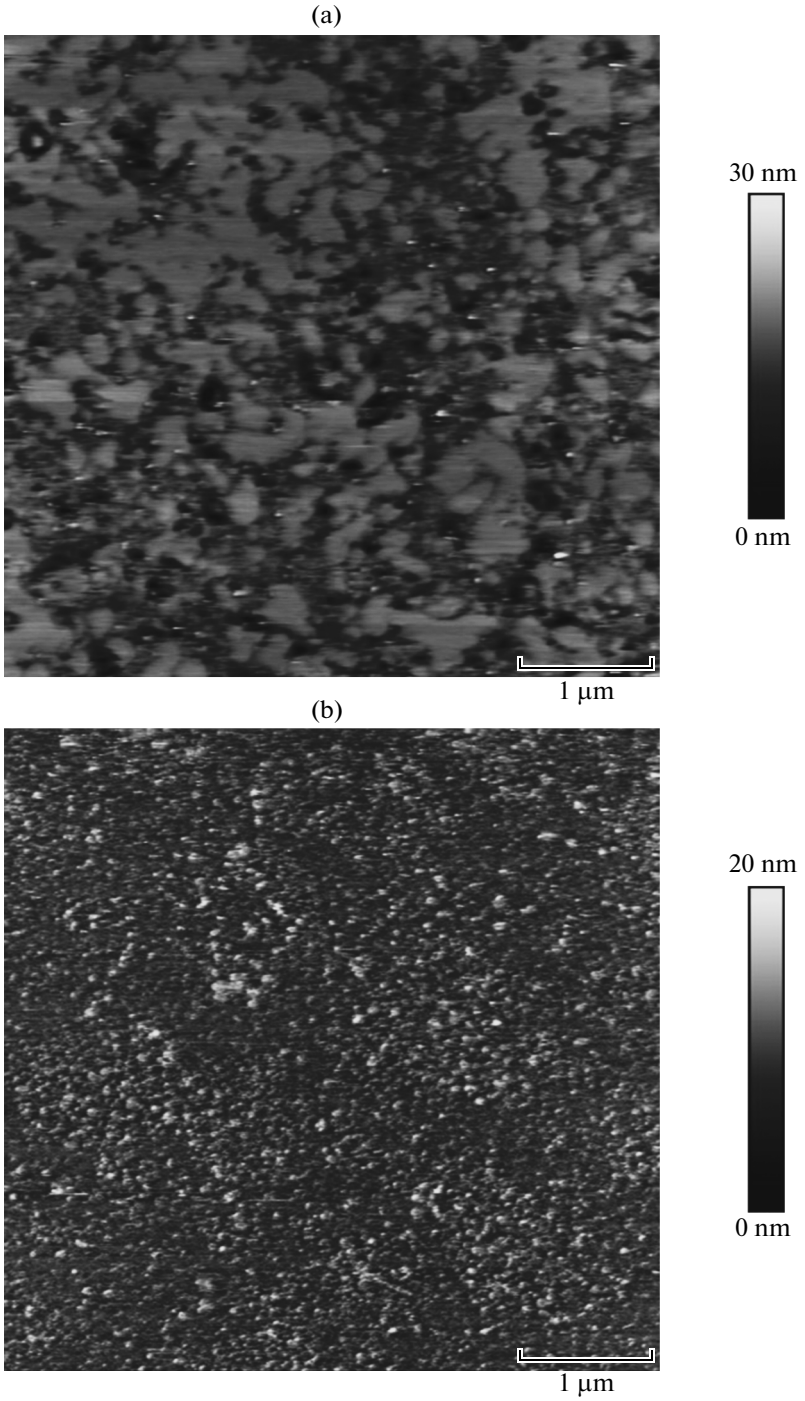

Fig. 5. Morphology detergent-resistant membrane domains isolated from human umbilical vein endothelial cells. The scan obtained on the mica surface by atomic force microscopy (Bruker). (a) Planar rafts; (b) caveolae. The height scale shows heights of the objects: lighter shades correspond to higher objects.

the intima due to diapedesis, this process being accompanied by cell activation and differentiation into tissue macrophages (Tall et al., 2012). Macrophages capture oxidized low-density lipoprotein (LDL) through the functioning of scavenger receptors, resulting in the formation of foam cells (Moore and Tabas, 2011). This is one of the main processes in the mechanism of atherosclerotic plaque formation. Changes in cholesterol homeostasis of monocytes have a direct impact on the formation of microdomains and their functions (Wolf et al., 2007). Also, it is an important fact that, under in vivo initiation of atherogenic lipo-

protein activation in patients with MI, not only the size and morphology of the DRMs are changed. The solubilization with detergent (Triton X-100) of the most major Fcγ-receptors (CD16, CD32, and CD64, some of them being involved in the atherogenic lipoprotein clearance), scavenger receptors (CD36, CD91, and CD163, involved in the capture of the modified LDL), integrins (CD11a, CD11b, and CD18), and the proteins anchored by glycosylphosphatidylinositol (CD14, CD47, and CD55) is much more difficult in the presence of MI in comparison with control, as shown in (Wolf et al., 2007). This means that the biochemical structure of the rafts changes significantly in the case of MI as well. These data are completely confirmed by the study (Salvary et al., 2012); it was found that the cholesterol level is higher in the planar rafts of the healthy donors (63 ± 3%) compared with the planar rafts isolated from monocytes of the patients with MI (41 ± 2%). Thus, a significant decrease in the size of the planar rafts during MI may be due to disturbance of the cholesterol metabolism in monocytes, which is accompanied by a decrease in cholesterol level in the rafts. In this case, the reduction in the solubilization with detergent of the major monocyte receptors, presumably, is the compensatory response of the cells which try to maintain their physiological functions in conditions of cholesterol deficiency and small raft sizes.

A different situation is observed for caveolae. According to our obtained data, there are statistically significant decrease in height and a slight decrease in their diameter when caveolae are extracted from monocytes of the patients with MI. Other authors (Salvary at al., 2012) have shown that cholesterol levels is lower in caveola fractions from healthy donors (13 ± 1%) than from patients with MI (34 ± 2%). These results do not contradict each other, if the fact shown in Fig. 4 is taken into account. Caveolae from the patients with MI (Figs. 4d, 4e) is smaller than caveolae from the healthy donors (Fig. 4c), but it is obvious that caveolae from the patients show a tendency to significant aggregation (Fig. 4d) and actually form a monolayer on the mica surface (Fig. 4e). Thus, the total area occupied by caveolae isolated from monocytes of the patients with MI is greater than the area occupied by caveolae isolated from the monocytes of the healthy donors and, therefore, it is logical to think that the total amount of cholesterol would be significantly higher. Therefore, here, as in the case of planar rafts, alteration of the morphology of submembranous structures reflects the deviation of their biochemistry.

Planar rafts and caveolae were isolated from HUVEC in the same manner as DRMs of monocytes. However, they differ significantly in the size and morphology. There are two possible explanations for the developed and irregular structure of HUVEC planar rafts. Either we observe the aggregation of the planar rafts during their isolation from HUVEC, or the developed structures on the mica surface reflect the real morphology of the planar rafts on the surfaces of living cells. The second explanation is most likely, since the AFM investigation of the planar rafts was performed immediately after the isolation. Furthermore, the concentration of the planar rafts was very high; they almost completely cover the surface of mica. It has been shown (Rinia et al., 2001), that the high concentration of cholesterol in the rafts leads to the formation of larger and irregular structures. In our experiments, the planar rafts isolated from HUVEC had the complex, large, and irregular shape; in addition, a microhardness test and elasticity mapping (data not shown) showed that these structures are highly rigid; i.e., they are likely to contain more cholesterol than do monocyte planar rafts. It can be thought that the morphological differences are caused by functional differences of the cells. Monocytes are highly mobile cells; they continually form, reorganize, combine, and disassemble the rafts. At the same time, endothelial cells are stationary and more stable; they practically act as a permanent functional platform for all the intravascular physiological processes. As a result, they form larger and more developed DRM structures.

The significant functional differences between the cells explain the significant differences in caveolae morphology as well: monocyte caveolae are involved in intracellular caveolae-dependent transport, whereas caveolae of endothelial cells are mostly involved in transcytosis.

The methodological part of this work clearly showed that the planar rafts and caveolae increase in size already at the second day of storage (table). Fast aggregation of the structures was observed in all cases. In our previous work, where the method of high-speed AFM was used, it was demonstrated that within 50 min of dynamic observation (video mode), there was an increase in the total surface of the planar rafts by 1.1 times (on the average, from 91000 to 102000 nm^2) (Pleskova et al., 2012). The excess of free energy at the interface is a driving force for merging of nanometer rafts into larger structures. Therefore, the main methodological conclusion is that it is necessary to obtain information on the actual size and shape of the planar rafts and caveolae immediately after isolation; otherwise, there are inevitable errors in the evaluation of either the size or form of DRMs.

Thus, we demonstrated a rapid aggregation of the planar rafts and caveolae. The following facts were showed for the structures studied at the first day after isolation: 1) planar rafts containing flotillin-1 as the main marker and caveolae containing caveolin-1 marker, have different sizes and morphology, 2) DRMs isolated from healthy donor monocytes, are different from the same structures of the patients with MI, and 3) planar rafts and caveolae isolated from different cells (monocytes and endothelial cells) differ morphologically and metrically.

ACKNOWLEDGMENTS

We thank Drs. R. Filomenko and T. Salvary for professional advice and technical assistance in the isolation and biochemical analysis of planar rafts and caveolae. This work was financially supported by the Regional Council of Burgundy and the Labex Action Integrated Smart System program.

REFERENCES

Dart, C., Lipid microdomains and the regulation of ion channel function, *J. Physiol.*, 2010, vol. 588, pp. 3169–3178.

de Almieda, R.F.M., Fedorov, A., and Prieto, M., Sphingomyelin/phosphatidylcholine/cholesterol phase diagram: boundaries and composition of lipid rafts, *Biophys. J.*, 2003, vol. 85, pp. 2406–2416.

Drevot, Ph., Langlet, C., Guo, X.-J., Bernard, A.-M., Colard, O., Chauvin, J.-P., Lasserre, R., and He, H.-T., TCR signal initiation machinery is pre-assembled and activated in a subset of membrane rafts, *EMBO J.*, 2002, vol. 21, pp. 1899–1908.

Gajate, C., Gonzalez-Camacho, F., and Mollinedo, F., Lipid raft connection between extrinsic and intrinsic apoptotic pathways, *Biochem. Biophys. Res. Commun.*, 2009, vol. 380, pp. 780–784.

Gajate, C. and Mollinedo, F., Lipid rafts and Fas/CD95 signaling in cancer chemotherapy, *Recent Patents Anti-Cancer Drug Discov.*, 2011, vol. 6, pp. 274–283.

Gohlke, A., Triola, G., Waldmann, H., and Winter, R., Influence of the lipid anchor motif of N-Ras on the interaction with lipid membranes: a surface plasmon resonance study, *Biophys. J.*, 2010, vol. 98, pp. 2226–2235.

Huang, L., Zhang, Y., Yu, Y., Sun, M., Li, Ch., Chen, P., and Mao, X., Role of lipid rafts in porcine reproductive and respiratory syndrome virus infection in MARC-145 cells, *Biochem. Biophys. Res. Commun.*, 2011, vol. 414, pp. 545–550.

Korade, Z. and Kenworthy, A.K., Lipid rafts, cholesterol and the brain, *Neuropharmacology*, 2008, vol. 55, pp. 1265–1273.

Levitan, I., Fang, Y., Rosenhouse-Dantsker, A., and Romanenko, V., Cholesterol and ion channels, *Subcell Biochem.*, 2010, vol. 51, pp. 509–549.

Marin, R., Marrero-Alonso, J., Fernandez, C., Cury, D., and Diaz, M., Estrogen receptors in lipid raft signalling complexes for neuroprotection, *Frontiers Biosci.*, 2012, vol. 4, pp. 1420–1433.

Melser, S., Molino, D., Batailler, B., Peypelut, M., Laloi, M., Wattelet-Boyer, V., Bellec, Y., Faure, J.-D., and Moreau, P., Links between lipid homeostasis, organelle morphodynamics and protein trafficking in eukaryotic and plant secretory pathways, *Plant Cell Rep.*, 2011, vol. 30, pp. 177–193.

Moore, K.J. and Tabas, I., The cellular biology of macrophages in atherosclerosis, *Cell*, 2011, vol. 145, pp. 341–355.

Pleskova, S.N., *Atomno-silovaya mikroskopiya v biologicheskikh i meditsinskikh issledovaniyakh* (Atomic-Force Microscopy in Biology and Medicine), Dolgoprudnyi: Intellekt, 2011.

Pleskova, S.N., and Pudovkina, E.E., Morphology and structural properties of rafts, *Cell Tissue Biol.*, 2013, vol. 7, no. 6, pp. 497–503.

Pleskova, S.N., Aybeke, E.N., Pudovkina, E.E., Bourillot, E., and Lesniewska, E., The study of monocytes and their submembrane structures by atomic force microscopy, *J. Biol. Phys. Chem.*, 2012, vol. 12, pp. 168–173.

Quinn, P.J. and Wolf, C., The liquid-ordered phase in membranes, *Biochim. Biophys. Acta*, 2009, vol. 1788, pp. 33–46.

Rinia, H.A., Snel, M.M.E., van der Eerden, J.P.J.M., and de Kruij, B., Visualizing detergent resistant domains in model membranes with atomic force microscopy, *FEBS Lett.*, 2001, vol. 501, pp. 92 – 96.

Salvary, T., Gambert-Nicot, S., Brindisi, M.C., Meneveau, N., Schiele, F., Séronde, M.F., Lorgis, L., Zeller, M., Cottin, Y., Kantelip, J.P., Gambert, P., and Davani, S., Pravastatin reverses the membrane cholesterol reorganization induced by myocardial infarction within lipid rafts in CD14(+)/CD16(–) circulating monocytes, *Biochim. Biophys. Acta*, 2012, vol. 1821, pp. 1287– 294.

Scuderi, M.R., Cantarella, G., Scollo, M., Lempereur, L., Palumbo, M., Saccani-Jotti, G., and Bernardini, R., The antimitogenic effect of the cannabinoid receptor agonist WIN55212-2 on human melanoma cells is mediated by the membrane lipid raft, *Cancer Lett.*, 2011, vol. 310, pp. 240–249.

Sheets, E.D., Holowka, D., and Baird, B., Critical role for cholesterol in Lyn-mediated tyrosine phosphorylation of FcεRI and their association with detergent-resistant membranes, *J. Cell Biol.*, 1999, vol. 145, pp. 877 – 887.

Smart, E.J., Graf, G.A., McNiven, M.A., Sessa, W.C., Engelman, J.A., Scherer, P.E., Okamoto, T., and Lisanti, M.P., Caveolins, liquid-ordered domains, and signal transduction, *Mol. Cell. Biol.*, 1999, vol. 19, pp. 7289–7304.

Sowa, G., Novel Insights into the role of caveolin-2 in cell- and tissue-specific signaling and function, *Biochem. Res. Int.*, 2011, p. 809259. doi:10.1155/2011/809259

Staubach, S. and Hanisch, F.-G., Lipid rafts: signaling and sorting platforms of cells and their roles in cancer, *Expert Rev. Proteomics*, 2011, vol. 8, pp. 263–277.

Tall, A.R., Yvan-Charvet, L., Westerterp, M., and Murphy, A.J., Cholesterol efflux a novel regulator of myelopoiesis and atherogenesis, *Arterioscler. Thromb. Vasc. Biol.*, 2012, vol. 32, pp. 2547–2552.

Wolf, Z., Orsó, E., Werner, T., Klünemann, H.H., and Schmitz, G., Monocyte cholesterol homeostasis correlates with the presence of detergent resistant membrane microdomains, *Cytometry*, 2007, vol. 71A, pp. 486–494.

Translated by D. Novikova